

---

---

CATALYSIS IN CHEMICAL  
AND PETROCHEMICAL INDUSTRY

---

---

# Structural and Electronic Properties of Highly Dispersed Particles of the Active Components of Pd/Al<sub>2</sub>O<sub>3</sub> Catalysts of Butadiene-1,3 Hydrogenation

A. V. Boretskaya<sup>a, \*</sup>, I. R. Ilyasov<sup>a, \*\*</sup>, and A. A. Lamberov<sup>b, \*\*\*</sup>

<sup>a</sup>Kazan (Volga) Federal University, Kazan, Tatarstan, 420008 Russia

<sup>b</sup>Butlerov Institute of Chemistry, Kazan State University, Kazan, Tatarstan, 420008 Russia

\*e-mail: ger-avg91@mail.ru

\*\*e-mail: ilildar@yandex.ru

\*\*\*e-mail: lamberov@list.ru

Received January 11, 2019; revised February 11, 2019; accepted February 15, 2019

**Abstract**—The effect of the acidic characteristics of an alumina support on the properties of formed palladium particles is studied to improve the activity of catalysts for the hydrogenation of unsaturated hydrocarbons of the pyrogasoline fraction. High catalytic activity is characteristic of highly dispersed palladium particles, but the surfaces of palladium particles are blocked by unsaturated hydrocarbons, due to their electron deficiency. In this work, palladium/alumina catalysts with supports of different acidities due to chemical modification with various reagents are studied via NH<sub>3</sub> temperature-programmed desorption, transmission electron microscopy, and X-ray photoelectron spectroscopy. The samples are subjected to catalytic tests in the butadiene-1,3 hydrogenation reaction under laboratory conditions. The catalysts on supports with acidic modifiers display low butadiene-1,3 conversion and higher selectivity toward butene-1, relative to an unmodified sample. The catalysts on the supports treated with basic additives displayed high butadiene-1,3 conversion while retaining their selectivities toward butene-1 and butane.

**Keywords:** butadiene hydrogenation,  $\gamma$ -Al<sub>2</sub>O<sub>3</sub> modification, NH<sub>3</sub> temperature-programmed desorption, transmission electron microscopy, X-ray photoelectron spectroscopy

**DOI:** 10.1134/S2070050419040032

## INTRODUCTION

The catalytic hydrogenation of diene hydrocarbons is used in industry at the first stage of the hydrogenation purification of the benzene–toluene fraction of pyrolysis and the purification of the butene fraction, since diene hydrocarbons are poisons for polymerization catalysts [1–6]. The catalysts used for the hydrogenation of such hydrocarbons are predominantly palladium/alumina systems with platinum contents of 0.2–0.5 wt % [7, 8]. They are characterized by better performance parameters at low temperatures than other supported metallic systems [9–11]. The catalysts become deactivated during hydrogenation due to the strong adsorption of unsaturated hydrocarbons on electron-deficient sites and the subsequent blocking of their working surfaces [12, 13]. The butadiene-1,3 hydrogenation reaction is structurally sensitive, and the composition of its products is governed by the structural and electronic properties of the highly dispersed active component, which is stabilized as a result of strong interaction with the support [14–16]. In considering its geometric characteristics in [17], it was

noted that the fraction of angular and edge metal atoms grows for small palladium particles (less than 8 nm in size).

There are different ways of synthesizing heterogeneous catalysts for the hydrogenation of unsaturated hydrocarbons. The authors of [18] synthesized platinum/alumina catalysts by mixing aluminum isopropoxide, block copolymer (P123), and hydrogen hexachloroplatinate(IV) in ethanol with subsequent thermal treatment at 400°C. This formed platinum particles encapsulated inside a mesostructural support. Such systems displayed high values (more than 90%) for the conversion of butadiene-1,3 and the selectivity of its conversion into butenes at 50°C.

In [19], palladium nanoparticles were synthesized from a complex of cetyltrimethylammonium bromide and sodium tetrachloropalladate(II). Maximum butadiene-1,3 conversion was observed at 20°C, but the reaction was conducted at an increased hydrogen pressure of 20 bar.

The authors of [20] studied  $\gamma$ -Al<sub>2</sub>O<sub>3</sub> supported copper- and palladium-based catalysts. Suspensions of

copper and platinum nanoparticles were preliminarily synthesized via chemical vapor deposition. The butadiene-1,3 conversion for these catalysts at 40°C was less than 20%.

High-percentage systems with a platinum content of 1.7 wt % were used by the authors of [3] in the butadiene-1,3 hydrogenation reaction, and palladium deposited onto palladium foil was used in [21].

Preparing catalytic systems with the use of more complicated means than impregnation will require additional engineering solutions for implementation on an industrial scale. Complication of the techniques used for the synthesis of catalytic systems will raise their own cost and therefore that of the final hydrocarbon product [22]. There is thus a need for synthesizing impregnated catalytic systems that are efficient in the butadiene-1,3 hydrogenation reaction.

The general mechanism behind the catalytic activity of supported palladium particles in the hydrogenation of unsaturated hydrocarbons is still unclear. It is therefore of interest to study the effect of the structural and electronic properties of nanosized palladium particles on their hydrogenating activity [23]. In this work, we studied palladium/alumina catalyst samples with supports ( $\gamma$ -Al<sub>2</sub>O<sub>3</sub>) of different acidities resulting from their chemical modification with different reagents. This approach offers the possibility of retaining the phase composition and textural characteristics of the support and thus tracing the change in the electronic properties of a catalyst's active component upon varying the acidic properties of alumina.

## EXPERIMENTAL

### *Sample Synthesis*

The initial compound used for synthesizing our alumina supports was aluminum monohydroxide powder (Sasol, Pural Sb). The acidic modifiers were acetic acid (10 wt %) and ammonium fluoride (0.5 wt % fluorine), and the basic modifiers were sodium hydroxide (0.5 wt % sodium) and cesium nitrate (3 wt %). The main criteria for selecting the nature and concentration of modifiers were the retention of the phase composition of an alumina support and a slight change in its textural characteristics. Acetic acid decomposes in synthesizing alumina and does not leave behind any additional impurity ions. There is thus great interest in using it as a modifier of alumina supports. Ammonium fluoride salt supplies an electronegative element (fluorine), and ammonium cations are eliminated in synthesizing a support, rather than being incorporated into it. Sodium hydroxide and cesium nitrate are sources of alkaline additives. It is of fundamental interest to use cesium in amounts of 3 wt % as the strongest base.

Aluminum hydroxide was treated with aqueous solutions of modifiers at 85°C and subsequently dried at 120°C. It then underwent isothermal treatment in

an air flow at 550°C. Unmodified alumina has a specific surface area of 233 m<sup>2</sup>/g and a porometric volume of 0.48 cm<sup>3</sup>/g; the differential curve of the pore volume distribution has a maximum at 6.8 nm, depending on the pore diameter. Our cesium-containing sample was calcined at 650°C. In this work, unmodified supports are denoted as Al<sub>2</sub>O<sub>3</sub>; the samples modified with acetic acid, fluorine, sodium, and cesium are designated Al<sub>2</sub>O<sub>3</sub>(Ac), Al<sub>2</sub>O<sub>3</sub>(F), Al<sub>2</sub>O<sub>3</sub>(Na), and Al<sub>2</sub>O<sub>3</sub>(Cs), respectively.

The catalysts were synthesized via the chemisorption impregnation of preliminarily evacuated supports, using palladium acetylacetonate from benzene. Each supported system was exposed for 2 h at 20°C. After the discolored solvent was removed, the samples were washed with a fresh amount of benzene and subsequently dried at 80°C. The content of palladium in the catalysts was 0.5 wt %. The resulting catalysts are denoted below as Pd/Al<sub>2</sub>O<sub>3</sub> (the catalyst on an unmodified support) and Pd/Al<sub>2</sub>O<sub>3</sub>(Ac), Pd/Al<sub>2</sub>O<sub>3</sub>(F), Pd/Al<sub>2</sub>O<sub>3</sub>(Na), and Pd/Al<sub>2</sub>O<sub>3</sub>(Cs) (the catalyst samples synthesized on the corresponding supports).

### *Analysis and Study of the Samples*

**Elemental composition** of the samples was studied on a Bruker S8 Tiger X-ray fluorescent wavelength dispersive spectrometer (Germany). The spectrometer was equipped with a rhodium X-ray tube having a power of 4 kW. The samples were ground into particles less than 10  $\mu$ m in size inside a planetary ball mill. Pressed pellets were placed into the spectrometer, where they were analyzed using the standardized Geoquant approach. Undetectable elements were estimated from the mass loss on calcination (LOC) up to 1100°C.

**Total acidity** of the alumina supports was determined via ammonia temperature-programmed desorption (NH<sub>3</sub> TPD) on an AutoChem 2950 HP analyzer. The mass of each sample loaded into the quartz reactor was 0.5 g. The samples were degassed at 550°C, and the heating rate was 10°C/min. The flow rate of the carrier gas (He) was 10 mL/min. The support was then saturated with a 10% NH<sub>3</sub>-He mixture at room temperature for 60 min and subsequently purged with argon at 100°C to remove the physically adsorbed ammonia. Analysis was done within the temperature range of 25–700°C. Dividing the measured curves into temperature regions corresponding to different energies of ammonia desorption allowed quantitative estimates of the contribution from weak (temperature of desorption  $T_d < 250^\circ\text{C}$ ), medium ( $250 \leq T_d < 350^\circ\text{C}$ ), and strong ( $T_d \geq 350^\circ\text{C}$ ) acidic sites [2].

**Morphological studies via transmission electron microscopy** were performed on a JEOL JEM 2010 electron microscope (Japan) with an accelerating volt-

**Table 1.** Elemental composition of our aluminum oxides and catalysts

Sample	Content of elements, wt %						LOC, %
	Al	Pd	F	Na	Cs	Fe	
Al <sub>2</sub> O <sub>3</sub>	94.811	—	—	0.001	—	0.005	5.042
Al <sub>2</sub> O <sub>3</sub> (Ac)	94.560	—	—	—	—	—	5.320
Al <sub>2</sub> O <sub>3</sub> (F)	94.003	—	0.528	—	—	0.007	4.853
Al <sub>2</sub> O <sub>3</sub> (Na)	94.438	—	—	0.462	—	0.003	5.017
Al <sub>2</sub> O <sub>3</sub> (Cs)	91.683	—	—	—	2.894	0.003	5.425
Pd/Al <sub>2</sub> O <sub>3</sub>	94.246	0.482	—	—	—	0.004	5.182
Pd/Al <sub>2</sub> O <sub>3</sub> (Ac)	93.772	0.514	—	—	—	—	5.608
Pd/Al <sub>2</sub> O <sub>3</sub> (F)	93.017	0.504	0.563	—	—	0.010	5.810
Pd/Al <sub>2</sub> O <sub>3</sub> (Na)	93.744	0.490	—	0.481	—	0.005	5.166
Pd/Al <sub>2</sub> O <sub>3</sub> (Cs)	90.933	0.514	—	—	3.01	0.003	5.460

age of 200 kV and an ultimate lattice resolution of 0.14 nm. Analysis was done using the carbon substrates of an UZD-1UCh2 ultrasonic disperser. Samples of the catalysts were subjected to preliminary thermal treatment at 400°C; specifically, oxidation with a 10% O<sub>2</sub>–He mixture (2 h), exposure for 10 min in an inert atmosphere, and reduction with a 10% H<sub>2</sub>–He mixture (2 h).

**Chemosorption titration with carbon monoxide (CO)** was conducted on our AutoChem 2950 HP analyzer after preliminarily treating the supported systems (in situ) by the means described above. The catalyst samples were saturated with carbon monoxide at room temperature. The dispersity of palladium particles was calculated as the ratio of the amount of surface palladium atoms to their total content in each sample. The concentration of palladium atoms was calculated assuming that one CO molecule was adsorbed on one palladium atom.

**X-ray photoelectron spectroscopic (XPS) studies** were performed on a KRATOS Analytical ES-300 spectrometer using a non-monochromatized MgK<sub>α</sub> X-ray source. All samples were evacuated to  $P = 10^{-7}$  mbar in the preliminary preparation chamber, where they were subjected to further pretreatment at 400°C. The samples were then subjected to evacuation at  $10^{-9}$  mbar. The spectrometer's energy scale was calibrated against the bonding energies of metallic gold ( $E_b(\text{Au}4f_{7/2}) = 84.0$  eV) and copper ( $E_b(\text{Cu}2p_{3/2}) = 932.7$  eV). The measured data were processed and the spectra were analyzed using the XPS CALC software in combination with standard graphic software suites. The spectra were decomposed into their components by approximating peaks from the sum of Lorentzian and Gaussian functions with Shirley background subtraction. The error in processing the spectra was less than 1%.

**Catalytic tests** of the synthesized samples in the butene-1,3 hydrogenation reaction were performed in

a laboratory flow-type setup with a fixed catalyst bed. The results presented below were obtained at a reaction temperature of 40°C and atmospheric pressure. The catalyst load was 0.05 g. Prior to tests, the samples were subjected to redox treatment at 400°C in the reactor. The feedstock flow rate was 1500 mL/h. Two mixtures of 10% butadiene-1,3 and 5% H<sub>2</sub> in argon were used as the initial reagents. The molar ratio of hydrogen to butadiene-1,3 in the reaction feedstock was 1.2 : 1. The initial feedstock and the reaction products were analyzed via gas chromatography on a Khromos GKh-1000 chromatograph. The conversion of butadiene-1,3 ( $K_{\text{butadiene}}$ ) was calculated as the ratio of the volume of converted butadiene-1,3 to the amount of it in the initial feedstock; i.e.,  $K = \Delta[\text{C}_4\text{H}_6] : [\text{C}_4\text{H}_6]_{\text{init}}$ , %. The selectivity of the conversion of butadiene-1,3 into butene-1 ( $S_{\text{butene}}$ ) was estimated as the ratio of the amount of butene-1 that formed to that of the converted butadiene-1,3; i.e.,  $S = \Delta[\text{C}_4\text{H}_8] : \Delta[\text{C}_4\text{H}_6]$ , %. The selectivity of butadiene-1,3 conversion into *n*-butane ( $S_{\text{butane}}$ ), *trans*- ( $S_{\text{trans-butene-2}}$ ), and *cis*-butenes-2 ( $S_{\text{cis-butene-2}}$ ) was determined in a similar manner.

## RESULTS AND DISCUSSION

The results from elemental analysis for the studied alumina and catalyst samples are presented in Table 1. Silicon, copper, and zinc impurities account for the remaining percentage of elemental content.

Preliminary modification with basic additives produced no notable changes in the phase composition or textural characteristics of the alumina supports [24].

According to the NH<sub>3</sub> TPD results, modifying a support with acidic additives increased the total acidity of corresponding samples Al<sub>2</sub>O<sub>3</sub>(Ac) and Al<sub>2</sub>O<sub>3</sub>(F), due mainly to raising the concentration of strong acidic (probably Brønsted) sites [2, 25, 26] (see Fig. 1

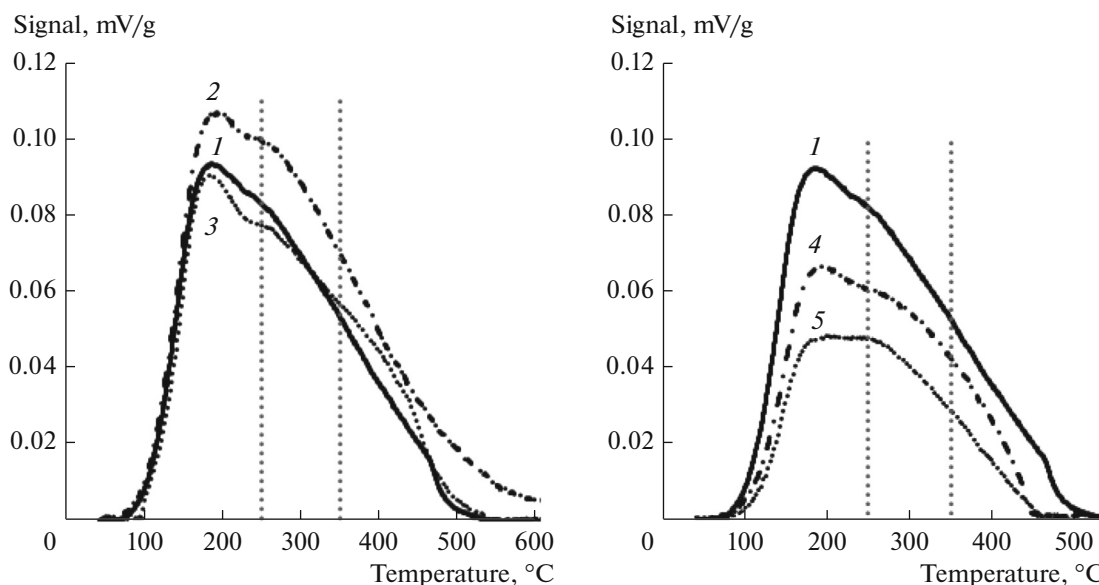


Fig. 1. TPD profile of aluminum oxides (1)  $\text{Al}_2\text{O}_3$ , (2)  $\text{Al}_2\text{O}_3(\text{Ac})$ , (3)  $\text{Al}_2\text{O}_3(\text{F})$ , (4)  $\text{Al}_2\text{O}_3(\text{Na})$ , and (5)  $\text{Al}_2\text{O}_3(\text{Cs})$ .

and Table 2). However, the reasons for their increased acidity were different. With sample  $\text{Al}_2\text{O}_3(\text{Ac})$ , it was due to the formation of a defective structure in  $\gamma\text{-Al}_2\text{O}_3$  upon the decomposition of basic aluminum acetate salts [27]. An increase in acidity was observed throughout the range of TPD profiles. The temperature of complete ammonia desorption also grew (from  $558^\circ\text{C}$  for  $\text{Al}_2\text{O}_3$  to  $688^\circ\text{C}$  for  $\text{Al}_2\text{O}_3(\text{Ac})$ ). A local 21% increase in acidity was observed for the  $\text{Al}_2\text{O}_3(\text{F})$  support in the  $350$  to  $470^\circ\text{C}$  range of temperatures. The temperature of complete desorption was left unchanged. The increase in the acidity of this sample was due to the effect of electronegative fluorine ions on the coordination spheres of aluminum cations [28]. The authors of [29] concluded that a less than 1 wt % content of fluorine atoms results in the terminal OH groups of a support being replaced by halide atoms.

Table 2. Number of acidic sites, according to  $\text{NH}_3$  TPD results\*

Sample	$\Sigma N$	Weak		Medium		Strong	
		$N$	$\Delta^{\text{rel}}$	$N$	$\Delta^{\text{rel}}$	$N$	$\Delta^{\text{rel}}$
$\text{Al}_2\text{O}_3$	819	369	—	246	—	204	—
$\text{Al}_2\text{O}_3, \text{Ac}$	1044	438	+19	313	+27	293	+44
$\text{Al}_2\text{O}_3, \text{F}$	853	350	-5	256	+4	247	+21
$\text{Al}_2\text{O}_3, \text{Na}$	552	254	-31	193	-22	105	-49
$\text{Al}_2\text{O}_3, \text{Cs}$	356	153	-59	132	-46	71	-65

\*  $\Sigma N$  is the total concentration of acidic sites,  $\mu\text{mol/g}$ ;  $N$  is the number of acidic sites of the corresponding rate,  $\mu\text{mol/g}$ ;  $\Delta^{\text{rel}}$  is the ratio of the increase/decrease in the number of acidic sites of the modified sample to their content in unmodified alumina within the corresponding rate, %.

Introducing basic additives into the composition of supports suppressed the strength and concentration of acidic sites, due to the predominant interaction between modifiers and Brønsted sites. This was accompanied by a drop in total acidity, from 819 to 552 and  $356 \mu\text{mol/g}$  for  $\text{Al}_2\text{O}_3(\text{Na})$  and  $\text{Al}_2\text{O}_3(\text{Cs})$ , respectively. The greatest drop in the concentration of acidic sites was observed upon introducing cesium, the basicity of which is higher. As we showed in [30], the atoms of alkali additives lower the concentration of acidic Lewis and Brønsted sites by being integrated into the coordinatively unsaturated sites of a support to replace the protons of acidic hydroxyl groups. The deposition of the active component's precursor onto supports of different acidities is accompanied by the formation of palladium particles with different sizes and charge states.

According to the electron microscopy data (Figs. 2a and 2b), the palladium particles in the  $\text{Pd}/\text{Al}_2\text{O}_3$  catalyst based on an unmodified support varied in size, from 5 to 20 nm. These were spherical particles with amorphized outer shells corresponding to oxidized palladium (PdO) and a metallic core with interplanar distance  $d_{200} = 0.192 \text{ nm}$ . In some cases (see Fig. 2c), metallic palladium particles with  $d_{111} = 0.224 \text{ nm}$  were also observed.

Modifying a support with alkaline additives did not produce any notable changes in the shape and size of deposited palladium particles (Figs. 3a and 3d).  $\text{Pd}/\text{Al}_2\text{O}_3(\text{Na})$  was also characterized by the presence of particles with oxidized shells (see Fig. 3b) and metallic palladium with interplanar distance  $d_{111} = 0.225 \text{ nm}$  (see Fig. 3c). Metallic palladium particles with interplanar distance  $d_{111} = 0.225 \text{ nm}$  were also observed on the surface of the  $\text{Pd}/\text{Al}_2\text{O}_3(\text{Cs})$  catalyst

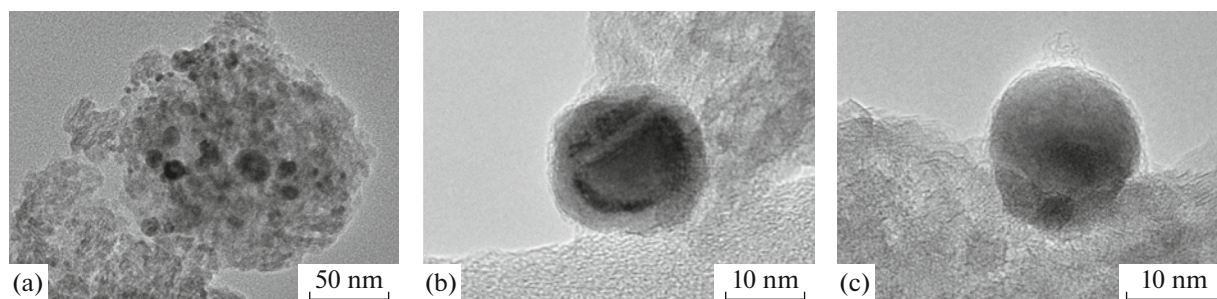


Fig. 2. TEM photos of the Pd/Al<sub>2</sub>O<sub>3</sub> catalyst.

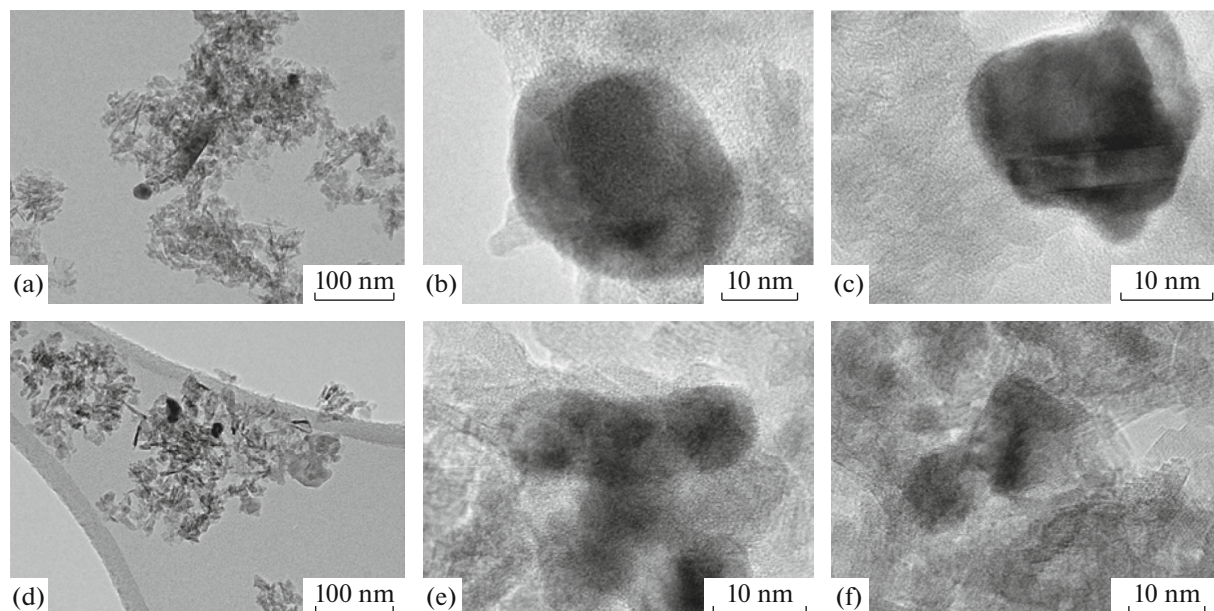


Fig. 3. TEM photos of the catalysts (a)–(c) Pd/Al<sub>2</sub>O<sub>3</sub>(Na) and (d)–(f) Pd/Al<sub>2</sub>O<sub>3</sub>(Cs).

(see Figs. 3e and 3f), but no palladium in the oxidized state was found.

In contrast to the earlier samples, the surfaces of the Pd/Al<sub>2</sub>O<sub>3</sub>(Ac) and Pd/Al<sub>2</sub>O<sub>3</sub>(F) catalysts based on supports with a high concentrations of acidic sites contained palladium in the form of clusters nearly 1 nm in size (Figs. 4a and 4c). The palladium particles of these samples had weak contrast on the surfaces of the supports. The presence of palladium was confirmed by the results from elemental analysis for the corresponding region (see Figs. 4b and 4d). This ultradisperse distribution of deposited particles was a result of their interacting with the strong acidic sites of the supports [31].

All our catalysts were characterized by high dispersities of palladium particles, estimated through the chemisorption titration of carbon monoxide (Table 3). The highest dispersity of palladium particles was characteristic of the Pd/Al<sub>2</sub>O<sub>3</sub>(Ac) sample prepared on the basis of the support with the highest acidity.

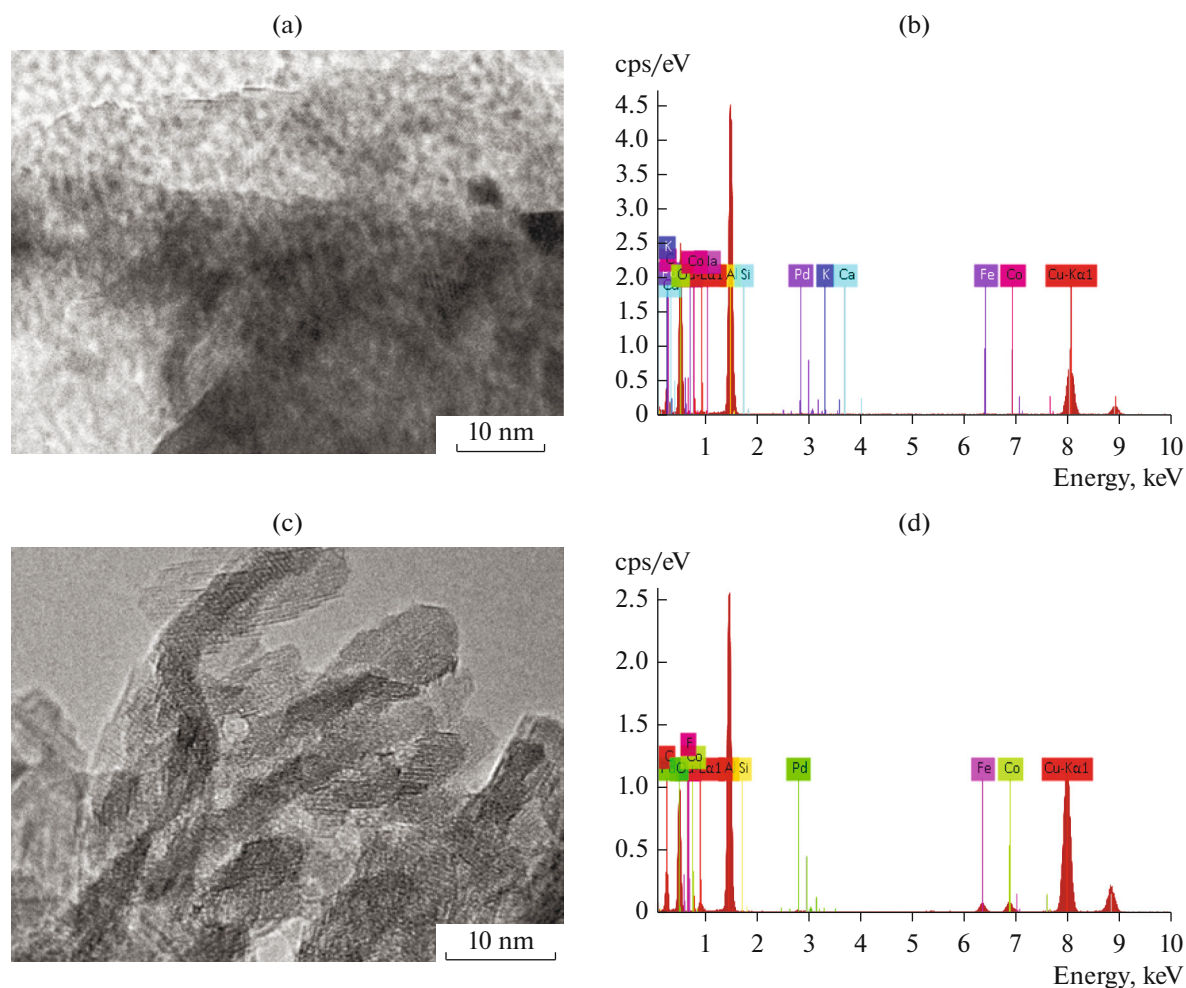
The electronic state of palladium in the studied catalysts was estimated via X-ray photoelectron spectroscopy (XPS). With the exception of Pd/Al<sub>2</sub>O<sub>3</sub>(Cs), we were able to distinguish two major charge states of

Table 3. Structural and electronic characteristics of the catalysts\*

Sample	$D_{Pd}$ , %	$d_{Pd}$ , %	$v(Pd^0)$ , %	$v(PdO)$ , %
Pd/Al <sub>2</sub> O <sub>3</sub>	82	5–20	72	28
Pd/Al <sub>2</sub> O <sub>3</sub> (Ac)	95	≈1	75	25
Pd/Al <sub>2</sub> O <sub>3</sub> (F)	89	≈1	70	30
Pd/Al <sub>2</sub> O <sub>3</sub> (Na)	84	5–30	91	9
Pd/Al <sub>2</sub> O <sub>3</sub> (Cs)	82	3–20	100	0

\* $D_{Pd}$  is the dispersity of palladium particles;  $d_{Pd}$  is the diameter of particles according to TEM results, nm;  $v(Pd^0)$  is the content of reduced palladium particles;  $v(PdO)$  is the content of oxidized palladium particles.





**Fig. 4.** (a), (c) TEM photos and (b), (d) EDX spectra of catalysts (a), (b) Pd/Al<sub>2</sub>O<sub>3</sub>(Ac) and (c), (d) Pd/Al<sub>2</sub>O<sub>3</sub>(F).

palladium in all our samples. The doublet with the Pd3d<sub>5/2</sub> bonding energy of 335.4 eV corresponds to the reduced form of palladium (Fig. 5). The doublet at 336.8 eV is typical of the palladium particles incorporated into the oxide PdO [2, 26, 32].

The Pd/Al<sub>2</sub>O<sub>3</sub> sample was characterized by the presence of 72% metallic and 28% oxidized palladium particles (see Table 3). The distribution of palladium particles over the surfaces of the Pd/Al<sub>2</sub>O<sub>3</sub>(Ac) and Pd/Al<sub>2</sub>O<sub>3</sub>(F) catalysts in the form of nanoclusters was not accompanied by any notable changes in the con-

tent of oxidized and reduced forms of palladium, relative to the Pd/Al<sub>2</sub>O<sub>3</sub> system. The proportions of the oxidized palladium phase in the composition of PdO on the surfaces of the Pd/Al<sub>2</sub>O<sub>3</sub>(Ac) and Pd/Al<sub>2</sub>O<sub>3</sub>(F) samples were 25 and 30%, respectively.

In the Pd/Al<sub>2</sub>O<sub>3</sub>(Na) and Pd/Al<sub>2</sub>O<sub>3</sub>(Cs) catalysts, the content of metallic palladium was observed to grow up to 91 and 100%, respectively, due to the low acidity of the corresponding supports.

The results from catalytic tests under the conditions of incomplete butadiene-1,3 conversion are

**Table 4.** Results from catalytic tests

Sample	$K_{\text{butadiene}}$ , %	$S_{\text{butene-1}}$ , %	$S_{\text{butane}}$ , %	$S_{\text{trans-butene-2}}$ , %	$S_{\text{cis-butene-2}}$ , %
Pd/Al <sub>2</sub> O <sub>3</sub>	64.2	34.6	30.4	28.1	6.9
Pd/Al <sub>2</sub> O <sub>3</sub> (Ac)	54.3	59.4	0.5	33.4	6.7
Pd/Al <sub>2</sub> O <sub>3</sub> (F)	27.9	53.0	0.5	38.0	8.5
Pd/Al <sub>2</sub> O <sub>3</sub> (Na)	80.8	26.1	34.7	28.9	10.3
Pd/Al <sub>2</sub> O <sub>3</sub> (Cs)	87.3	32.5	23.2	34.6	9.7

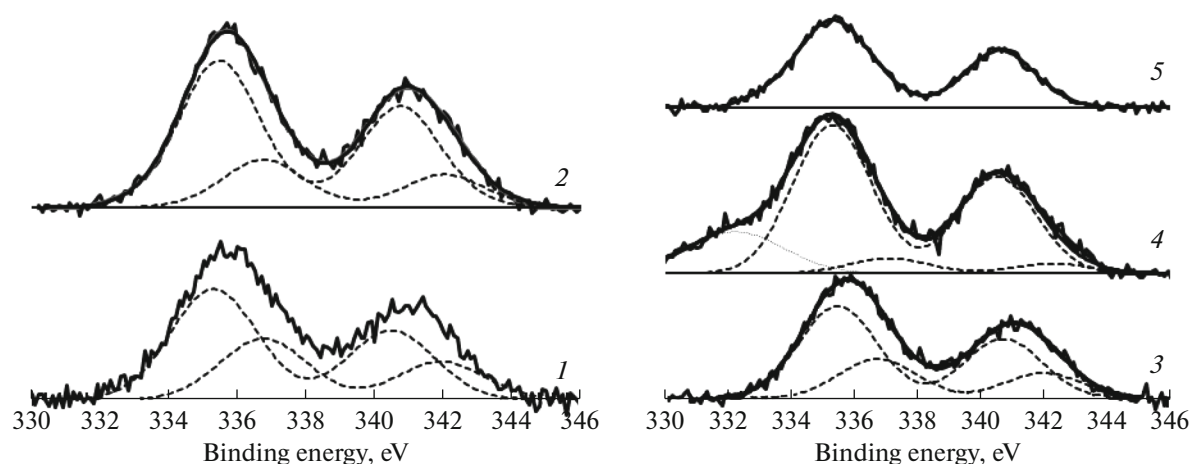


Fig. 5. XPS results for catalysts (1) Pd/Al<sub>2</sub>O<sub>3</sub>, (2) Pd/Al<sub>2</sub>O<sub>3</sub>(Ac), (3) Pd/Al<sub>2</sub>O<sub>3</sub>(F), (4) Pd/Al<sub>2</sub>O<sub>3</sub>(Na), and (5) Pd/Al<sub>2</sub>O<sub>3</sub>(Cs).

given for these samples in Table 4. The lowest degrees of butadiene-1,3 conversion (54.3 and 27.9%, respectively) and high selectivity toward butene-1 were obtained for Pd/Al<sub>2</sub>O<sub>3</sub>(Ac) and Pd/Al<sub>2</sub>O<sub>3</sub>(F), but their selectivity toward butane was less than 1%. These catalysts and unmodified Pd/Al<sub>2</sub>O<sub>3</sub> were characterized by close contents of the oxidized and reduced forms of palladium, but also by smaller palladium particles. We may assume that the weak butadiene-1,3 conversion on the Pd/Al<sub>2</sub>O<sub>3</sub>(Ac) and Pd/Al<sub>2</sub>O<sub>3</sub>(F) samples was a result of structural factors [21, 33–35]. The single-site adsorption of diene with subsequent 1,2-inclusion of hydrogen atoms is in this case possible [33]. The presence of fluorine in the support results in the coordination unsaturation of deposited palladium particles. We noted that the Pd/Al<sub>2</sub>O<sub>3</sub>(F) sample was characterized by a higher content of oxidized palladium particles, relative to the other systems (see Table 3). There was strong chemisorption of hydrocarbons and the blocking of active sites on the surfaces of electron-deficient palladium particles, reducing the hydrogenating activity of the Pd/Al<sub>2</sub>O<sub>3</sub>(F) sample [36, 37].

High butadiene-1,3 conversion was attained on the Pd/Al<sub>2</sub>O<sub>3</sub>(Na) and Pd/Al<sub>2</sub>O<sub>3</sub>(Cs) catalytic systems, but the changes in the selectivities to butene-1 and butane were negligible in comparison to the unmodified catalyst. The increased hydrogenating activity was apparently due to the readsorption of molecules of olefin hydrocarbons with their subsequent hydrogenation to butane.

All our catalysts displayed strong selectivity toward *trans*-butene-2. The highest value was observed for the Pd/Al<sub>2</sub>O<sub>3</sub>(F) catalyst (see Table 3).

## CONCLUSIONS

We studied the structural and electronic properties of the active components of palladium/alumina cata-

lysts whose supports had identical compositions and textural characteristics but different acidities.

It was shown that modifying the supports with basic additives results in the formation of palladium particles of nearly the same size as that of particles on an unmodified sample, but the concentrations of reduced forms of palladium on them were higher. A sample of catalyst was synthesized that contained palladium only in the reduced state and displayed stronger butadiene-1,3 conversion than the other studied systems.

Treating a support with acidic modifiers reduces the size of palladium particles from 30 to 1 nm while retaining the electronic state typical of the catalyst on an unmodified support. Such palladium clusters display high selectivity toward butene-1, due to the single-site adsorption of butadiene-1,3.

## FUNDING

This work was by supported by a subsidy granted to Kazan (Volga) Federal University to improve its competitiveness among the world's leading scientific and educational centers.

## REFERENCES

1. Moyes, R.B., Wells, P.B., Grant, J., and Salman, N.Y., *Appl. Catal., A*, 2002, vol. 229, nos. 1–2, pp. 251–259.
2. Bhogeswararao, S. and Srinivas, D., *J. Catal.*, 2015, vol. 327, pp. 65–77.
3. Lonergan, W.W., Xing, X., Zheng, R., Qi, S., Huang, B., and Chen, J.G., *Catal. Today*, 2011, vol. 160, no. 1, pp. 61–69.
4. Benkhaled, M., Descorme, C., Duprez, D., Morin, S., Thomazeau, C., and Uzio, D., *Appl. Catal., A*, 2008, vol. 346, nos. 1–2, pp. 36–43.
5. Silvestre-Albero, J., Rupprechter, G., and Freund, H.-J., *Chem. Commun.*, 2006, no. 1, pp. 80–82.

6. Silvestre-Albero, J., Borasio, M., Rupprechter, G., and Freund, H.-J., *Catal. Commun.*, 2007, vol. 8, no. 3, pp. 292–298.
7. Derrien, M.L., *Stud. Surf. Sci. Catal.*, 1986, vol. 27, pp. 613–666.
8. Ouchaib, T., Massardier, J., and Renouprez, A., *J. Catal.*, 1989, vol. 119, no. 2, pp. 517–520.
9. Mittendorfer, F., Thomazeau, C., Raybaud, P., and Toulhoat, H., *J. Phys. Chem. B*, 2003, vol. 107, no. 44, pp. 12287–12295.
10. Kang, J.H., Shin, E.W., Kim, W.J., Park, J.D., and Moon, S.H., *J. Catal.*, 2002, vol. 208, no. 2, pp. 310–320.
11. Khan, N.A., Shaikhutdinov, S., and Freund, H.-J., *Catal. Lett.*, 2006, vol. 108, nos. 3–4, pp. 159–164.
12. Stakheev, A.Yu. and Kustov, L.M., *Appl. Catal., A*, 1999, vol. 188, nos. 1–2, pp. 3–35.
13. Hub, S., Hilaire, L., and Touroude, R., *Appl. Catal.*, 1988, vol. 36, pp. 307–322.
14. Boitiaux, J.P., Cosyns, J., and Robert, E., *Appl. Catal.*, 1987, vol. 35, no. 2, pp. 193–209.
15. Tardy, B., Noupa, C., Leclercq, C., Bertolini, J.C., Houreau, A., Treilleux, M., Faure, J.P., and Nihoul, G., *J. Catal.*, 1991, vol. 129, no. 1, pp. 1–11.
16. Valden, M., Lai, X., and Goodman, D.W., *Science*, 1998, vol. 281, no. 5383, pp. 1647–1650.
17. Mohr, C. and Claus, P., *Sci. Prog.*, 2001, vol. 84, no. 4, pp. 311–334.
18. Zhang, Z., Zhu, Y., Asakura, H., Zhang, B., Zhang, J., Zhou, M., Han, Y., Tanaka, T., Wang, A., Zhang, T., and Yan, N., *Nat. Comm.*, 2017, vol. 8. <https://www.nature.com/articles/ncomms16100>. Cited October 8, 2019.
19. Berhault, G., Bisson, L., Thomazeau, C., Verdon, C., and Uzio, D., *Appl. Catal., A*, 2007, vol. 327, no. 1, pp. 32–43.
20. Lucci, F.R., Liu, J., Marcinkowski, M.D., Yang, M., Allard, L.F., Flytzani-Stephanopoulos, M., and Sykes, E.C.H., *Nat. Comm.*, 2015, vol. 6. <https://www.nature.com/articles/ncomms9550>. Cited October 8, 2019.
21. Gaube, J. and Klein, H.-F., *Appl. Catal., A*, 2014, vol. 470, pp. 361–368.
22. Guseva, L., *Plastik*, 2015, no. 3, pp. 16–20.
23. Delage, M., Didillon, B., Huiban, Y., Lynch, J., and Uzio, D., *Stud. Surf. Sci. Catal.*, 2000, vol. 130, pp. 1019–1024.
24. Boretskaya, A.V., Il'yasov, I.R., Lamberov, A.A., and Laskin, A.I., *Russ. J. Appl. Chem.*, 2017, vol. 90, no. 2, pp. 161–168.
25. Yashnik, S.A., Kuznetsov, V.V., and Ismagilov, Z.R., *Chin. J. Catal.*, 2018, vol. 39, no. 2, pp. 258–274.
26. Dai, Q., Zhu, Q., Lou, Y., and Wang, X., *J. Catal.*, 2018, vol. 357, pp. 29–40.
27. Borisevich, Yu.P., Fomichev, Yu.V., and Levinter, M.E., *Zh. Fiz. Khim.*, 1982, vol. 56, no. 5, pp. 1298–1299.
28. Paukshtis, E.A., *Infrakrasnaya spektroskopiya v geterogennom kislotno-osnovnom katalize (Infrared Spectroscopy in Heterogeneous Acid-Base Catalysis)*, Novosibirsk: Nauka, 1992.
29. Contescu, C., Contescu, A., Schramm, C., Sato, R., and Schwartz, J.A., *J. Colloid Interface Sci.*, 1994, vol. 165, no. 1, pp. 66–71.
30. Lamberov, A.A., Khalilov, I.F., Il'yasov, I.R., Bikmurzin, A.Sh., and Gerasimova, A.V., *Vestn. Kazan. Tekhnol. Univ.*, 2011, no. 13, pp. 24–35.
31. Saifullin, R.S., *Fizikokhimiya neorganicheskikh polimernykh i kompozitsionnykh materialov (Physical Chemistry of Inorganic Polymeric and Composite Materials)*, Moscow: Khimiya, 1990.
32. Chesnokov, V.V., Prosvirin, I.P., Zaitseva, N.A., Zaikovskii, V.I., and Molchanov, V.V., *Kinet. Catal.*, 2002, vol. 43, no. 6, pp. 838–846.
33. Miegge, P., Rousset, J.L., Tardy, B., Massardier, J., and Bertolini, J.C., *J. Catal.*, 1994, vol. 149, no. 2, pp. 404–413.
34. Narayanan, R. and El-Sayed, M.A., *J. Am. Chem. Soc.*, 2004, vol. 126, no. 23, pp. 7194–7195.
35. Silvestre-Albero, J., Rupprechter, G., and Freund, H.-J., *J. Catal.*, 2005, vol. 235, no. 1, pp. 52–59.
36. Bragin, O.V. and Liberman, A.L., *Prevrashcheniya uglevodorodov na metalsoderzhashchikh katalizatorakh (Conversion of Hydrocarbons on Metal-Containing Catalysts)*, Moscow: Khimiya, 1981.
37. Bursian, N.R., *Tekhnologiya izomerizatsii parafinovykh uglevodorodov (Isomerization Technology for Paraffin Hydrocarbons)*, Leningrad: Khimiya, 1985.

Translated by E. Glushachenkova